were obtained at 62.9 MHz on a Bruker WM250 spectrometer. The solid-state ^{13}C NMR spectra of **2** was obtained using cross-polarization magic angle spinning (CPMAS) on a crystalline sample. The sample was packed into an alumina rotor under a nitrogen atmosphere and acquired at 50.3 MHz on a Bruker MSL200 spectrometer. Spinning rates were approximately 4000–4500 Hz. Methyl and quaternary carbon resonances were assigned with the delay without decoupling pulse sequence of Opella and Frey.[11] Adamantane was used as an external reference, having chemical shifts of 29.50 ppm (*C*H) and 38.56 ppm (*C*H_2) with respect to tetramethylsilane.[19]

The solution absorption spectra of **2** was obtained at 21 °C with the use of a Hewlett-Packard 8451A diode-array spectrophotometer. A concentration of approximately 10^{-5} M in benzene was employed. The solid-state absorption spectra of **2** was obtained on microcrystalline samples by the method of Kobayashi et al.[20] A thin layer of freshly crystallized iminium salt was placed on a quartz slide. A similar slide or one coated with KBr was used as a reference.

Determination of Crystal Structures. Collection of Data. Crystals of the imine **1** and iminium salt **2** suitable for X-ray diffraction techniques were obtained from distillation of diethyl ether into an acetonitrile solution of each salt at about −20 °C. Each crystal was sealed in a Lindemann tube for data collection.

The space group of each compound was determined through precession photography. These showed that crystals were monoclinic and that the space group for each was $P2_1/c$. Accurate unit-cell parameters were determined from a least-squares fit of χ, ϕ, and 2θ. For **1**, 15 reflections where $18.6° < 2\theta < 25.9°$ were used. In **2**, a range of $19.6° < 2\theta < 31.3E$ was used for 15 reflections. Radiation was graphite monochromated Mo Kα, $\lambda = 0.71069$, and reflection intensities were measured with a Syntex $P2_1$ diffractometer having a coupled θ(crystal)–2θ(counter) scan. Selection of scan rates and initial data treatment have been previously described.[21] Corrections for Lorentz–polarization factors were made, but not for absorption. This will make the maximum error in F_o of 1.0% in **1** and 1.3% in **2**. All crystal data are summarized in Table IV.

Solution of Structures. In the iminium salt **2**, the coordinates of the chlorine atoms were found from a three-dimensional Patterson synthesis. All other atoms were located from three-dimensional electron-difference syntheses by use of a series of full-matrix least-squares refinements. The chlorine atom in the imine **1** was found by direct methods on 164 reflections with $|E| > 1.1$, and 20 sets of starting phases. All remaining atoms were found from the subsequent difference map. Refinement of the coordinates of all non-hydrogen atoms by full-matrix least-squares, which minimized $\Sigma\omega(|F_o| - |F_c|)^2$, was terminated when the maximum shift/error was 0.1. Throughout each refinement, scattering curves were taken from those in the International Tables.[22] Secondary extinction corrections were applied from SHELX. Positional parameters for non-hydrogen atoms of both structures are found in Tables II and III.

Acknowledgment. Technical assistance of R. Faggiani is gratefully acknowledged.

Supplementary Material Available: Tables of atomic positional parameters, anisotropic temperature factors, hydrogen positional parameters, and bond lengths and angles involving hydrogen atoms (8 pages); listings of observed (F_o) and calculated (F_c) reflection intensities (26 pages). Ordering information is given on any current masthead page.

(19) Earl, W. L.; Vander Hart, D. L. *J. Magn. Reson.* **1982**, *48*, 35–54.
(20) Kobyashi, H.; Vanagawa, Y.; Osada, H.; Minima, S.; Shiziwa, M. *Bull. Chem. Soc. Jpn.* **1972**, *46*, 1471–1479.
(21) (a) Lippert, B.; Lock, C. J. L.; Rosenberg, B.; Zvagulis, M. *Inorg. Chem.* **1977**, *16*, 314–319. (b) Hughes, R. P.; Krishnamachari, N.; Lock, C. J. L.; Powell, J.; Turner, G. *Inorg. Chem.* **1977**, *16*, 1525–1529.
(22) Cormer, D. T.; Waber, J. T. In *International Tables for X-ray Crystallography*; Ibers, J. A., Hamilton, W. C., Eds.; Kynoch Press: Birmingham, England, 1974; p 99.

NMR Study of Kinetic HH/HD/DD Isotope, Solvent, and Solid-State Effects on the Double Proton Transfer in Azophenine

Helmut Rumpel and Hans-Heinrich Limbach*

Contribution from the Institut für Physikalische Chemie der Universität Freiburg i.Br. Albertstrasse 21, D-7800 Freiburg, West Germany. *Received June 24, 1988*

Abstract: Azophenine (AP, *N,N'*-diphenyl-3,6-bis(phenylimino)-1,4-cyclohexadiene-1,4-diamine) is subject in liquid solution to a fast intramolecular double proton transfer involving two degenerate tautomers. Rate constants of this reaction have been measured as a function of temperature by applying different methods of dynamic NMR spectroscopy to various isotopically labeled AP species dissolved in different organic solvents. The rate constants do not depend on the dielectric constant of the solvent, which was varied between 2 (toluene) and 25 (benzonitrile). For $C_2D_2Cl_4$ as solvent, the full kinetic HH/HD/DD isotope effects were obtained at different temperatures. The observed kinetic isotope effects of $k^{HH}/k^{HD} = 4.1$ and $k^{HD}/k^{DD} = 1.4$ at 298 K indicate a breakdown of the rule of the geometric mean. ^{15}N CPMAS NMR experiments on crystalline azophenine showed that the reaction also takes place in the solid state. However, the degeneracy of the tautomerism is lifted in this phase because of intermolecular interactions. The mechanism of this reaction is discussed in detail, especially with respect to the questions of whether tunneling is involved and whether one or two protons are transferred in the rate-limiting step. The kinetic isotope effects can best be explained in terms of a stepwise consecutive single proton transfer mechanism involving either a highly polar zwitterion or an apolar singlet–biradical as intermediate. The observation that solvent effects on the reaction rates are absent and that the activation entropy of the reaction almost vanishes excludes the formation of a strongly solvated zwitterionic intermediate. Static medium effects on the double minimum potential of the proton transfer are discussed, taking into account previous results of IR experiments on AP and of solid-state NMR experiments on double proton transfers in organic glasses.

In the past years there has been a particular interest in neutral multiple hydrogen transfer reactions[1] where at least two protons, hydrogen atoms, or hydride ions are transferred between heavy atoms. Intramolecular[2-9] as well as intermolecular[10-14] multiple proton transfers have been studied. The fact that ions are not

(1) Since neither protons nor other ions are educts or products in these reactions, only the term hydrogen transfer would be correct, which includes the possibility of the transfer of protons, hydrogen atoms, or hydride ions; however, since protons are, generally, transferred in hydrogen-bonded systems we will use the term proton transfer.
(2) Limbach, H. H. The Use of NMR Spectroscopy in the Study of Hydrogen Bonding in Solution. In *Aggregation Processes*; Gormally, J., Wyn-Jones, E., Eds.; Elsevier: Amsterdam, 1983; Chapter 16.
(3) Limbach, H. H.; Hennig, J.; Gerritzen, D.; Rumpel, H. *Faraday Discuss. Chem. Soc.* **1982**, *74*, 822.
(4) Hennig, J.; Limbach, H. H. *J. Am. Chem. Soc.* **1984**, *106*, 292.

0002-7863/89/1511-5429$01.50/0

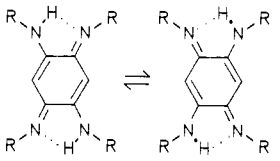

Figure 1. Azophenine tautomerism. I (azophenine,[54] AP): R = C_6H_5; Ia: R = [p-^{13}C]C_6H_5; Ib: R = C_6H_5, N = ^{15}N; Ic: R = C_6D_5, N = ^{15}N; II: R = H.

involved in these reactions makes them less sensitive to solvent effects and, thus, easier to treat theoretically than the usual ionic proton transfer reactions. As a consequence, neutral proton transfers can take place not only in the liquid but also in the solid state[15-26] and can be induced at cryogenic temperatures by light.[27-30] In organic and biochemical systems these processes are related to bifunctional catalysis and biological activity.[31-40]

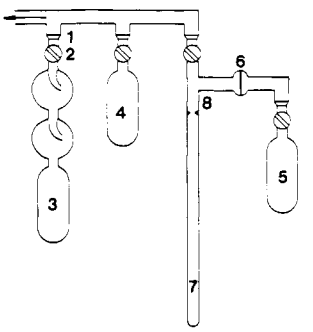

Figure 2. Glass apparatus for preparing NMR samples. Key: 1, Glass joint; 2, needle valve with Teflon stopcocks; 3, solent storage container; 4 and 5, glass vessels; 6, glass frit; 7, NMR tube; 8, place for seal off.

On the other hand, these reactions are an old topic of the theory of primary kinetic hydrogen/deuterium isotope effects[3,13,34,38-43] and of general theoretical chemistry.[44-53] For multiple concerted proton transfer reaction the so-called rule of the geometric mean (RGM) has been derived by combination of the equilibrium isotope effect[42] and transition-state theories.[40,42,43] This rule states, for example, for the rate constants k^{HH}, k^{HD}, k^{DD} of a symmetric double hydrogen/deuterium transfer reaction that

$$k^{HD} = (k^{HH}k^{DD})^{1/2}, \text{ i.e., } k^{HH}/k^{HD} = k^{HD}/k^{DD} \qquad (1)$$

The validity of this rule has been used in order to extract information about the number of protons in flight during the rate-limiting step of enzyme reactions from measurements of reaction rates as a function of the deuterium fraction in the mobile proton sites.[30-38]

In order to test eq 1 experimentally, NMR stratagems[3,12-14] have been described to determine k^{HH}, k^{HD}, and k^{DD} of symmetric inter- and intramolecular reactions. Measurements of such complete sets of kinetic isotope effects revealed, however, a breakdown of the RGM. E.g., for the 1:1 proton exchange between acetic acid and methanol in tetrahydrofuran[3,13] and for the intramolecular proton tautomerism of *meso*-tetraphenylporphine (TPP)[3] it was found that replacement of the first H atom by D resulted in a stronger decrease of the reaction rates than re-

(5) Schlabach, M.; Wehrle, B.; Limbach, H. H.; Bunnenberg, E.; Knierzinger, A.; Shu, A. Y. L.; Tolf, B. R.; Djerassi, C. *J. Am. Chem. Soc.* **1986**, *108*, 3856.

(6) Otting, G.; Rumpel, H.; Meschede, L.; Scherer, G.; Limbach, H. H. *Ber. Bunsenges. Phys. Chem.* **1986**, *90*, 1122.

(7) Bren, V. A.; Chernoivanov, V. A.; Konstantinovskii, L. E., Nivorozhkin, L. E.; Zhdanov, Y. A.; Minkin, V. I. *Dokl. Akad. Nauk SSSR* **1980**, *251*, 1129.

(8) Graf, F. *Chem. Phys. Lett.* **1979**, *62*, 291.

(9) Limbach, H. H.; Gerritzen, D. *Faraday Discuss. Chem. Soc.* **1982**, *74*, 279.

(10) Limbach, H. H.; Seiffert, W. *Ber. Bunsenges. Phys. Chem.* **1974**, *78*, 641.

(11) Limbach, H. H.; Seiffert, W. *J. Am. Chem. Soc.* **1980**, *102*, 538.

(12) Gerritzen, D.; Limbach, H. H. *Ber. Bunsenges. Phys. Chem.* **1981**, *85*, 527.

(13) Gerritzen, D.; Limbach, H. H. *J. Am. Chem. Soc.* **1984**, *106*, 869.

(14) Meschede, L.; Gerritzen, D.; Limbach, H. H. *Ber. Bunsenges. Phys. Chem.* **1988**, *92*, 469.

(15) Limbach, H. H.; Hennig, J.; Kendrick, R. D.; Yannoni, C. S. *J. Am. Chem. Soc.* **1984**, *106*, 4059.

(16) Limbach, H. H.; Gerritzen, D.; Rumpel, H.; Wehrle, B.; Otting, G.; Zimmermann, H.; Kendrick, R. D.; Yannoni, C. S. In *Photoreaktive Festkörper*; Sixl, H., Friedrich, J., Bräuchle, C., Eds.; M. Wahl Verlag: Karlsruhe, 1985; pp 19-43.

(17) Kendrick, R. D.; Friedrich, S.; Wehrle, B.; Limbach, H. H.; Yannoni, C. S. *J. Magn. Reson.* **1985**, *65*, 159.

(18) Meier, B. H.; Storm, C. B.; Earl, W. L. *J. Am. Chem. Soc.* **1986**, *108*, 6072.

(19) Limbach, H. H.; Wehrle, B.; Zimmermann, H.; Kendrick, R. D.; Yannoni, C. S. *J. Am. Chem. Soc.* **1987**, *109*, 929.

(20) Limbach, H. H.; Wehrle, B.; Zimmermann, H.; Kendrick, R. D.; Yannoni, C. S. *Angew. Chem.* **1987**, *99*, 241; *Angew. Chem., Int. Ed. Engl.* **1987**, *26*, 247.

(21) Wehrle, B.; Limbach, H. H.; Köcher, M.; Ermer, O.; Vogel, E. *Angew. Chem.* **1987**, *99*, 914; *Angew. Chem., Int. Ed. Engl.* **1987**, *26*, 934.

(22) Wehrle, B.; Zimmermann, H.; Limbach, H. H. *Ber. Bunsenges. Phys. Chem.* **1987**, *91*, 941; Wehrle, B.; Limbach, H. H.; Zimmermann, H. *J. Am. Chem. Soc.* **1988**, *110*, 7014.

(23) Nagoka, S.; Terao, T.; Imashiro, F.; Saika, A.; Hirota, N.; Hayashi, S. *Chem. Phys. Lett.* **1981**, *80*, 580; *J. Chem. Phys.* **1983**, *79*, 4694.

(24) Meier, B. J.; Graf, F.; Ernst, R. R. *J. Chem. Phys.* **1982**, *76*, 767.

(25) Graf, F.; Meyer, R.; Ha, T. K.; Ernst, R. R. *J. Chem. Phys.* **1981**, *75*, 2914.

(26) Benz, S.; Haeberlen, U.; Tegenfeldt, J. *J. Magn. Reson.* **1986**, *66*, 125.

(27) Völker, S.; van der Waals, J. H. *Mol. Phys.* **1976**, *32*, 1703. Voelker, S.; Macfarlane, R. *IBM Res. Develop.* **1979**, *23*, 547.

(28) Friedrich, J.; Haarer, D. *Angew. Chem.* **1984**, *96*, 96; *Angew. Chem., Int. Ed. Engl.* **1986**, *23*, 113.

(29) Moerner, W. E. *J. Mol. Electron.* **1986**, *1*, 55.

(30) Kämpff, G. *Ber. Bunsenges. Phys. Chem.* **1985**, *89*, 1179.

(31) Swain, C. G.; Brown, J. F. *J. Am. Chem. Soc.* **1952**, *74*, 2534; *Ibid.* **1952**, *74*, 2538.

(32) Ek, M.; Ahlberg, P. *Chem. Scr.* **1980**, *16*, 62.

(33) Engdahl, K. A.; Bivehed, H.; Ahlberg, P.; Saunders, W. H., Jr. *J. Chem. Soc., Chem. Commun.* **1982**, 423.

(34) Elrod, J. P.; Gandour, R. D.; Hogg, J. L.; Kise, M.; Maggiora, G. M.; Schowen, R. L.; Venkatasubban, K. S. *Faraday Symp. Chem. Soc.* **1975**, *10*, 145.

(35) Gandour, R. D.; Schowen, R. L. *Transition States of Biochemical Processes*; Plenum Press: New York, 1978.

(36) Hermes, J. D.; Cleland, W. W. *J. Am. Chem. Soc.* **1984**, *106*, 7263.

(37) Hermes, J. D.; Morrical, S. W.; O'Leary, M. H.; Cleland, W. W. *Biochemistry* **1984**, *23*, 5479.

(38) Belasco, J. G.; Albery, W. J.; Knowles, J. R. *Biochemistry* **1986**, *25*, 2529; *Ibid.* **1986**, *25*, 2552.

(39) Gross, P.; Steiner, H.; Krauss, F. *Trans. Faraday Soc.* **1936**, *32*, 877. Hornell, J. C.; Butler, J. A. V. *J. Chem. Soc.* **1936**, 1361.

(40) Gold, V. *Trans. Faraday Soc.* **1960**, *56*, 255; *Adv. Phys. Org. Chem.* **1969**, *7*, 259.

(41) Kresge, A. J. *Pure Appl. Chem.* **1964**, *8*, 243.

(42) Bigeleisen, J. *J. Chem. Phys.* **1955**, *23*, 2264.

(43) Albery, W. J.; Limbach, H. H. *Faraday Discuss. Chem. Soc.* **1982**, *24*, 291.

(44) Albery, W. J. *J. Phys. Chem.* **1986**, *90*, 3773.

(45) Brickmann, J.; Zimmermann, H. *Ber. Bunsenges. Phys. Chem.* **1966**, *70*, 157; *Ibid.* **1966**, *70*, 521; *Ibid.* **1967**, *71*, 160. Brickmann, J.; Zimmermann, H.; *J. Chem. Phys.* **1969**, *50*, 1608.

(46) Schuster, P., Zundel, G., Sandorfy, C., Eds. *The Hydrogen Bond*; North Holland Publishing Co.: Amsterdam, 1976.

(47) Bell, R. P. *The Tunnel Effect in Chemistry*; Chapman and Hall: London, 1980.

(48) Sarai, A. *J. Chem. Phys.* **1982**, *76*, 5554; *Ibid.* **1984**, *80*, 5341.

(49) Bersuker, G. I.; Polinger, V. Z. *Chem. Phys.* **1984**, *86*, 57.

(50) Limbach, H. H.; Hennig, J. *Chem. Phys.* **1979**, *71*, 3120. Limbach, H. H.; Hennig, J.; Stulz, J. *J. Chem. Phys.* **1983**, *78*, 5432. Limbach, H. H. *J. Chem. Phys.* **1984**, *80*, 5343.

(51) Siebrand, W.; Wildman, T. A.; Zgierski, M. Z. *J. Am. Chem. Soc.* **1984**, *106*, 4083; *Ibid.* **1984**, *106*, 4089. Smedarchina, Z.; Siebrand, W.; Wildman, T. A. *Chem. Phys. Lett.* **1988**, *143*, 395.

(52) Dewar, M. J. S.; Merz, K. M. *J. Mol. Struct. (THEOCHEM)* **1985**, *124*, 183; *Ibid.* **1983**, *87*, 3826.

(53) Merz, K. M.; Reynolds, C. H. *J. Chem. Soc., Chem. Commun.* **1988**, *90*.

placement of the second H atom by D. A similar breakdown of the RGM was recently observed in enzymatic reactions.[36,37] This effect can be interpreted in terms of either a concerted double proton transfer in the presence of tunnel effects[3,13,36] or a stepwise double proton transfer over the barrier.[3,36,38,44]

In order to know whether the breakdown of the RGM in double proton transfer reactions is general, i.e., not limited to the particular examples described so far, we have been engaged in a program of measuring complete sets of kinetic isotope effects in well-defined multiple proton transfer reactions using dynamic NMR spectroscopy. In this paper we report the results of a kinetic study of the tautomerism of azophenine[54] (AP, I; Figure 1), a dye that was first synthesized in 1875 by Kimich.[55] The constitution of AP, which is one of the oxidation products of aniline,[56] was established by Hepp et al.[57] As shown in Figure 1, this dye is able to form two degenerate tautomers. In a preliminary study[3] it was shown that the tautomerism of AP can be followed by dynamic NMR spectroscopy of suitably isotopically labeled AP. Thus, preliminary rate constants k^{HH} of the HH process in AP have been obtained. The parent compound II (Figure 1) is the nitrogen analogue of 2,6-dihydroxybenzoquinone, for which a similar tautomerism involving oxygen atoms has been established.[7,8] AP was studied here (i) because II is insoluble in inert organic solvents and (ii) because of the ease of introducing suitable spin labels such as ^2H, ^{15}N, and ^{13}C into AP. These labels allowed us not only to establish the purely intramolecular character of the tautomerism in Figure 1 but also to measure its kinetic HH/HD/DD isotope effects via a combination of ^1H and ^{13}C NMR spectroscopic methods. In order to know whether and how the environment influences the AP, tautomerism rate constants were measured for a variety of solvents. In addition, high-resolution ^{15}N solid-state NMR experiments were performed on the crystalline compound. The results of all experiments are reported here after the Experimental Section in which the synthesis of isotopically labeled AP, the sample preparation, and the conditions under which the NMR experiments were performed are described. The results are then discussed with respect to the question of how the transfer of the two protons in AP and related compounds takes place. For this purpose additional information on the proton dynamics in AP obtained recently by IR and NIR spectroscopy is taken into account.[58]

Experimental Section

Preparation of NMR Samples of AP Non-Deuterated and Deuterlated in the NH Sites. The sealed NMR samples of AP dissolved in organic solvents had to be prepared very carefully in order to exclude air and moisture and other impurities that might catalyze the proton exchange. For this purpose we used a glass apparatus attached to a vacuum line as shown in Figure 2. Greaseless Teflon needle valves (2) were employed to separate the different devices from the vacuum line. For the preparation of the samples, AP was placed in the glass vessel 5 which was then evacuated. If an NMR sample was to be prepared with AP deuterated in the NH sites, the following deuteration procedure was included. From attached solvent storage containers pure dried chloroform (four parts) and an H_2O/D_2O (one part) mixture with the desired deuterium fraction were condensed successively on AP in the vessel 5. AP dissolved completely in the chloroform phase. The mixture was then stirred magnetically for 1 h, after which the two solvents were evacuated. The use of pure H_2O during this procedure, which was repeated twice, had no effect on the NMR spectra of AP and was, therefore, omitted when non-deuterated samples were prepared. Attempts to deuterate AP with deuterated methanol or ethanol failed because AP reacts with these compounds. AP probably forms adducts with alcohols and, possibly, also with water. The concentration of the latter in $CHCl_3$ is, however, so low that hydrated AP was not observed here.

The following procedure was used for all NMR samples. After extensive evacuation, the pure degassed NMR solvent was condensed from the solvent container 3 into the vessel 5, the glass frit 6, and the NMR tube 7 in order to remove residual water and chloroform from the glass walls and from AP. After evaporation 0.5 mL of the NMR solvent was condensed on the solid AP. After separation from the vacuum line by closing the appropriate valve, the saturated solution was filtered via the glass frit 6 into the NMR tube, which was then sealed off at 8. During this procedure the tube was cooled to 77 K.

Synthesis of Azophenine (AP, I). At the beginning of our study we thought that the most convenient way of synthesizing AP and isotopically labeled AP would be the oxidation of aniline.[56] During the course of our studies, however, we found out by NMR that this would not produce the pure compound even if the oxidation products are purified by chromatography. As shown by ^{13}C NMR, there are at least three further byproducts with structures closely related to the structure of AP; i.e., the impurities are also subject to a similar tautomerism as AP. For this reason AP was synthesized from tetraaminobenzene (TAB) and aniline. The first step consists of the oxidation of TAB to II (Figure 1) with $FeCl_3$ in H_2O according to Nietzki et al.[59] AP is then easily obtained by reaction of II with aniline.[60] This process was carried out in the glass vessel 4 (Figure 2). Aniline (1 mL) was condensed on a mixture of 20 mg of II (0.15 mmol) and 78.6 mg (0.6 mmol) of aniline hydrochloride placed in 4. After the valve between the vacuum line and the glass vessel was closed, the suspension was heated under stirring to 130 °C during 30 min. Unreacted aniline was then removed by evaporation. The solid residue was dissolved in dichloromethane and purified via chromatography over silica, with dichloromethane as solvent. AP was found in the first fraction, in which no impurities could be detected either by chromatography, NMR, or mass spectroscopy. The red crystals were dried in vacuo: fp 236 °C (lit.[56] fp 236–237 °C); yield, 9% (6 mg); mass spectrum, m/e 440 (M^+), 439, 361, 348, 347, 256, 220, 219, 181, 142, 116, 89, 77, and 51.

Synthesis of Isotopically Labeled AP. Isotopically labeled AP was prepared from unlabeled II and from isotopically labeled aniline. For the ^1H NMR experiments we synthesized Ib and Ic (Figure 1). The latter was deuterated to ~99% in the four phenyl rings. The ^{15}N content of Ib and of Ic was 95%. For the ^{13}C NMR experiments it was necessary to synthesize Ia (Figure 1), specifically labeled in the para positions of the phenyl rings, to ~90% with the ^{13}C isotope. The synthesis of aniline-p-^{13}C has been described by Rumpel et al.[61] Aniline-^{15}N and pentadeuteroaniline-^{15}N were synthesized as described by Otting et al.[6]

Purification of Solvents. The solvents were condensed from vessel 4 into vessel 3, which contained an appropriate drying agent. Anthracene/sodium–potassium alloy was employed as drying agent for tetrahydrofuran-d_8 (THF) and toluene-d_8, and highly activated basic alumina (ICN, W2000) for deuterated chlorinated NMR solvents. All solvents were purchased with the exception of benzonitrile-d_5, which was prepared by analogy to the procedure described for the unlabeled compound[62] from aniline-d_7 by Sandmeyer reaction in DCl/D_2O. The product was dried over potassium–sodium alloy in a way similar to the other solvents. However, since benzonitrile reacts slowly with this alloy, after the liquid had turned red the solvent was removed from this drying agent by condensation into another vessel where the benzonitrile-d_5 was stored over basic alumina.

NMR Measurements. The ^1H and the ^{15}N CPMAS NMR spectra were measured with a pulse FT NMR spectrometer, Bruker CXP 100, working at 90.02 MHz for protons and 9.12 MHz for ^{15}N. Some ^1H NMR spectra and the ^{13}C NMR spectra were measured with a Bruker CXP 300 spectrometer working at 300.13 MHz for protons. The sample temperatures were calibrated before and after the NMR measurements with a PT 100 resistance thermometer (Degussa), embedded in an NMR tube, and are estimated accurate to ~0.5 °C. The temperature stability during the measurements was, however, better than 0.2 °C. The spectra were transferred from the Bruker Aspect 2000 minicomputer to a personal computer (Olivetti M28) and then to the Univac 1108 computer of the Rechenzentrum der Universität Freiburg via a direct data line. Kinetic and thermodynamic parameters were obtained by simulation of the spectra, as described below. Various experimental data were fitted to theoretical curves by a nonlinear least-squares fit program.[63]

NMR Line Shape Analysis. As shown in Results, we can interpret all dynamic NMR spectra of AP in terms of the well-known asymmetric two-state exchange problem, which will be shortly reviewed in this section. Consider a molecule exchanging between two unequally populated

(54) Abbreviations: **1**, 3,6-diimino-1,4-cyclohexadiene-1,4-diamine; **2**, *N,N'*-diphenyl-3,6-bis(phenylimino)-1,4-cyclohexadiene-1,4-diamine, (azophenine, AP); see also Figure 1.

(55) Kimich, C. *Chem. Ber.* **1875**, *8*, 1028.
(56) Ostrogovitch, A.; Silbermann, T. *Chem. Zentralbl.* **1908**, *79I*, 266.
(57) Fischer, O.; Hepp, B. *Chem. Ber.* **1888**, *21*, 681.
(58) Rumpel, H.; Limbach, H. H.; Zachmann, G. *J. Phys. Chem.* **1989**, *93*, 1812.
(59) Nietzki, R.; Hagenbach, E. *Chem. Ber.* **1887**, *20*, 328.
(60) Grünwälder, P. In *Houben-Weyl*, Thieme: Stuttgart, 1980; Vol. 7/3b, p 322.
(61) Rumpel, H.; Limbach, H. H. *J. Labelled Compd.* **1987**, *24*, 235.
(62) Vogel, A. I. *Elementary Practical Organic Chemistry*, 2nd ed.; Longman: Birmingham, AL, 1966.
(63) Marquardt, W. Share Distribution Center, Program No. 1428, 1964.

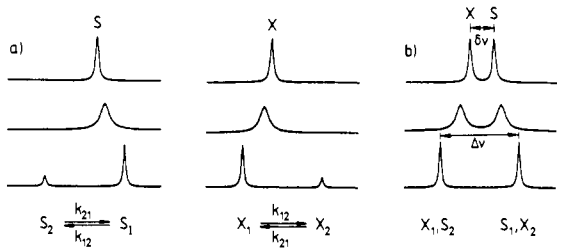

Figure 3. Calculated spectra for two single spins S and X located in an asymmetric two-state exchange system. The equilibrium constant $K_{12} = k_{12}/k_{21}$ was set to a value of 0.54 in all spectra. The values of k_{12} increase from the bottom to the top. For further explanation see text. (a) Spectra calculated for the case that the chemical shifts of all nuclei are different; (b) spectra calculated for the case where S and X are in similar chemical environments, i.e., for the validity of eq 4. (Adapted from ref 22.)

states 1 and 2 characterized by the probabilities x_1 and x_2. The equilibrium constant is then given by

$$K_{12} = x_1/x_2 = k_{12}/k_{21} \tag{2}$$

k_{12} and k_{21} are the rate constants of the exchange. Let the molecule contain two uncoupled spins A and X characterized by the chemical shifts ν_{A_1}, ν_{A_2}, ν_{X_1}, and ν_{X_2}, where the subscript indicates the molecule state. The exchange problem can then be formulated in terms of two superposed independent asymmetric two-state exchange systems A and X, for which the exchange-broadened line shapes are well-known. Either the modified Bloch equations,[64] Kubo–Sack,[65] or density matrix theory[66] can be used for their calculation. The result is shown in Figure 3a. In the slow-exchange regime each spin system contributes two lines to the spectrum, i.e., four lines appear at positions given by the chemical shifts of A and X in the two states, i.e., at ν_{A_1}, ν_{A_2}, ν_{X_1}, and ν_{X_2}. The line intensity ratios A_2/A_1 and X_2/X_1 correspond to the equilibrium constant K_{12}. As k_{12} is increased, the lines broaden and coalesce. The position of the averaged line S is given by

$$\nu_S = x_1\nu_{S_1} + (1 - x_1)\nu_{S_2},\ S = A, X \tag{3}$$

Thus, from the line possition in the fast exchange the equilibrium constant K_{12} can be obtained if the chemical shifts are known. In Figure 3b we consider a special case where

$$\nu_{A_1} = \nu_{X_2} \text{ and } \nu_{A_2} = \nu_{X_1} \tag{4}$$

In the slow-exchange regime, the spectra then contain only two lines A_1, X_2 and X_1, A_2 of equal intensity which broaden and sharpen again as k_{12} is increased. In this fast-exchange regime, the splitting $\delta\nu = \nu_A - \nu_X$ between the two averaged lines A and X is reduced and given by[15,16,22]

$$\delta\nu = \Delta\nu(1 - K_{12})/(1 + K_{12}) \tag{5}$$

where $\Delta\nu = \nu_{A_1} - \nu_{A_2} = \nu_{X_2} - \nu_{X_1}$ is the splitting in the slow-exchange regime. For the symmetrical case where $K_{12} = 1$, it follows that $\delta\nu = 0$, i.e., lines A and X coincide.

A homemade computer program handling all types of NMR exchange problems was used to calculate the spectra in Figure 3.

Results

This section contains the experimental results of our NMR measurements on AP in different organic solvents and in the solid state. Rate constants are obtained not only by NMR line shape analysis but also by magnetization transfer experiments in the rotating frame.[67] We first report ^{13}C NMR experiments by which the kinetic HH/DD isotope effects were obtained. We then show how the kinetic HH/HD isotope effects were determined via ^1H NMR spectroscopy. This method is also used for the study of solvent effects. Finally, high-resolution solid-state ^{15}N NMR spectra of AP are reported as a function of temperature.

^{13}C NMR Spectroscopy of ^{13}C-Enriched Azophenine in $C_2D_2Cl_4$. Line Shape Analysis. Figure 4 shows the superposed experimental and calculated NMR signals of the p-^{13}C atoms of Ia (see Figure

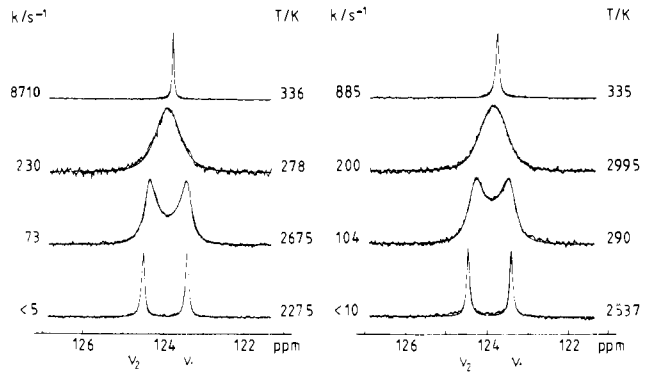

Figure 4. Superposed experimental and calculated 75.47-MHz ^{13}C NMR signals of the isotopically enriched (90%) p-^{13}C atoms of Ia dissolved in $C_2D_2Cl_4$ as a function of temperature. Left, deuterium fraction in the NH sites $D = 0$, right, $D = 0.99$. A total of 200–4000 scans on the average, 90° pulses, 5-s repetition time, broad-band decoupling power 2 W.

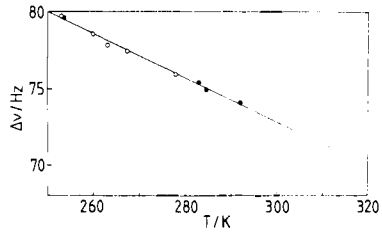

Figure 5. Dependence of $\Delta\nu$ as a function of temperature in $C_2D_2Cl_4$. (○) Ia-H_2; (●) Ia-D_2.

1) dissolved in $C_2D_2Cl_4$ as a function of temperature at a deuterium fraction of $D = 0$ and $D = 1$ in the NH sites. At low temperatures the slow-exchange regime is reached, with two sharp signals of equal intensities indicating that eq 4 is fulfilled. As the temperature is raised the lines broaden and finally coalesce into one sharp line. This spectral pattern indicates a symmetric exchange process with $\delta\nu = 0$, i.e., $K_{12} = 1$ in eq 5. Thus, we can drop the distinction between A and X nuclei and write in the following $\Delta\nu = \nu_1 - \nu_2$. We tentatively assign the high-field line ν_1 to the phenyl ring attached to the NH unit and the low-field line ν_2 to the phenyl ring attached to the =N—atom of AP. Since the kinetic results are not affected by this assignment, no further attempts to confirm this assignment were undertaken. Figure 4 also shows that the exchange becomes much slower as the molecule is deuterated in the NH sites; the coalescence point is raised ~20 K. This observation of a kinetic hydrogen/deuterium isotope effect of the exchange is consistent with the fact that the two carbon atoms can only exchange by a proton transfer process during which the two degenerate tautomers in Figure 1 are interconverted. The line shape calculations were performed in terms of the usual symmetric two-state exchange with a homemade general computer program for intra- and intermolecular exchange. For the calculations it is necessary to know the values of $\Delta\nu$ in the fast-exchange limit. As shown in Figure 5, the values of $\Delta\nu$ obtained in the slow-exchange region depend linearly on temperature, with

$$\Delta\nu = -0.14T + 115.8 \text{ Hz} \tag{6}$$

at 75.47 MHz. Within the margin of error of our experiments there is no detectable difference between the values of Ia-H_2 and Ia-D_2. A further problem associated with the method of line shape analysis, i.e., the determination of the line widths W_0 in the absence of exchange, is addressed in a subsequent section.

^{13}C NMR Polarization Transfer Experiments in the Rotating Frame. It is well-known that in the slow-exchange regime line shape analysis is not very accurate. In order to overcome this difficulty, we performed polarization transfer experiments in the rotating frame according to a method described previously.[67] The method is especially simple if neither scalar nor dipolar coupled spins are involved, and if the exchange problem is symmetric, i.e.,

(64) Gutowsky, H. S.; McCall, D. W.; Slichter, C. P. *J. Chem. Phys.* **1953**, *21*, 279.
(65) Kubo, R. *Nuovo Cimento, Suppl.* **1957** *6*, 1063. Sack, R. A. *Mol. Phys.* **1958**, *1*, 163.
(66) Binsch, G. *J. Am. Chem. Soc.* **1969**, *91*, 1304.
(67) Hennig, J.; Limbach, H. H. *J. Magn. Reson.* **1982**, *49*, 322.

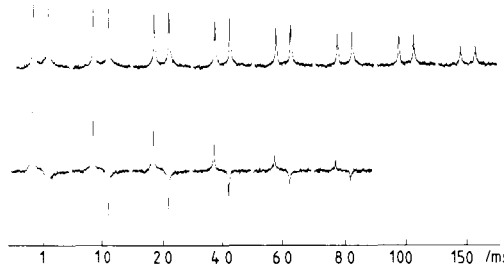

Figure 6. A 75.47-MHz ^{13}C NMR magnetization transfer experiment in the rotating frame on a la-D_2 in $C_2D_2Cl_4$ at 265 K and a deuterium fraction in the NH sites of $D = 0.99$. Upper spectral set, experiment I; lower spectral set, experiment II.

if $k_{12} = k_{21} = k$. As shown in Figure 6, two types of experiments are, as a rule, performed. In experiment I, where a spin-locking pulse is applied along the y axis of the rotating frame immediately after a $(\pi/2)_x$ pulse, the polarizations of the exchanging spins are parallel and decay exponentially with the longitudinal relaxation time in the rotating frame, $T_{1\rho}$

$$S = S(0)\ \exp(-t/T_{1\rho}), \quad S = A, X \tag{7}$$

In eq 7 it is assumed that $T_{1\rho}$ is equal for both spins or that the difference has been averaged out by the exchange. In experiment II the polarizations are prepared in an antiparallel way with a delay $\tau = 1/(2\Delta\nu)$ between the two pulses; the exchange between the polarizations is given by[67]

$$S = S(0)\ \exp(-1/T_{1\rho} + 2k), \quad S = A, X, A(0) = -X(0) \tag{8}$$

Since $k_{12} = k_{21} = k$, both polarizations have the same decay constant $1/T_{1\rho} + 2k$. Thus, k can easily be obtained from the difference of the polarization decay in experiments I and II, as shown in Figure 6, in a region where line shape analysis is not accurate.

^1H NMR Experiments on ^{15}N-Enriched Azophenine in $C_2D_2Cl_4$. Line Shape Analysis. The process of an intramolecular double proton transfer in AP is further confirmed by ^1H NMR experiments on the ^{15}N-enriched compounds Ib and Ic (Figure 1). Most experiments were performed on the latter in order to avoid interference between the proton signals in the ^1H–^{15}N sites and the aromatic proton signals. Figure 7 shows the superposed experimental and calculated ^1H NMR signals of the ^1H–^{15}N units of Ic dissolved in $C_2D_2Cl_4$ as a function of temperature. Preliminary spectra of this type have been presented previously.[3] At low temperatures the proton signal consists of a doublet with the frequencies $\nu + {}^1J_{^1H^{15}N}/2$ and $\nu - {}^1J_{^1H^{15}N}/2$, because of coupling of the hydrogen-bonded proton to one ^{15}N atom. Since ^{15}N has the spin $^1/_2$ it can exist in the spin states, α or β, leading to the observed doublet. At high temperatures the signal has a triplet structure. This observation means that the NH proton is now equally coupled to two ^{15}N atoms. The switch from the doublet to the triplet splitting is expected for an intramolecular pathway of the proton transfer, i.e., the case where the proton always jumps between the same two ^{15}N atoms,[6] which can be in any one of the spin states $\alpha\alpha$, $\alpha\beta$, $\beta\alpha$, and $\beta\beta$. Thus, the following reactions take place:

$$N(\alpha)\text{–}H\cdots N(\alpha) \rightleftharpoons N(\alpha)\cdots H\text{–}N(\alpha) \tag{9}$$

$$N(\alpha)\text{–}H\cdots N(\beta) \rightleftharpoons N(\alpha)\cdots H\text{–}N(\beta) \tag{10}$$

$$N(\beta)\text{–}H\cdots N(\alpha) \rightleftharpoons N(\beta)\cdots H\text{–}N(\alpha) \tag{11}$$

$$N(\beta)\text{–}H\cdots N(\beta) \rightleftharpoons N(\beta)\cdots H\text{–}N(\beta) \tag{12}$$

Protons reacting according to eq 9 and 12 do not change their transition frequencies and, therefore, always contribute sharp line components at $\nu \pm {}^1J_{^1H^{15}N}/2$. Protons switching between ^{15}N atoms in the spin states α and β according to eq 10 and 11 also give in the slow-exchange range sharp line components at $\nu \pm {}^1J_{^1H^{15}N}/2$; but when the exchange becomes faster, these line components broaden, coalesce, and eventually give rise to one sharp line in the center of the signal, i.e., a triplet appears. The ratio

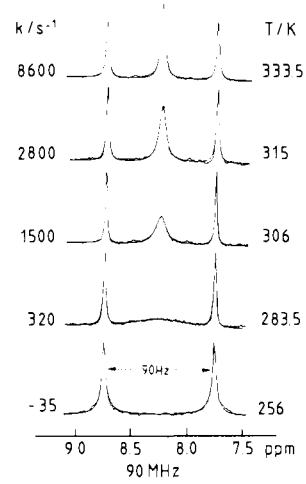

Figure 7. Superposed experimental and calculated 90.02-MHz ^1H NMR signals of the ^1H–^{15}N units of Ic dissolved in $C_2D_2Cl_4$ at a deuterium fraction $D = 0$ in the NH sites as a function of temperature. A total of 200–500 scans, 60° pulses, 3-s repetition time. k is the rate constant of the tautomerism.

of the integrated intensities of the inner exchange-broadened line component to each of the outer line components is always 2:1; however, the peak heights behave in this way only at very high temperatures, where the inner line component no longer shows line broadening; i.e., a peak height ratio of less then 2:1 is, therefore, indicative that the extremely fast exchange has not yet been reached.

The line shapes in Figure 7 were calculated in terms of a superposition of a symmetric two-state exchange and two nonexchanging one-state systems. We used a similar computer program as for the calculation of the ^{13}C NMR spectra shown in Figure 4. The advantage of the line shape analysis in Figure 7 as compared to Figure 4 is that no assumptions concerning W_0 and the change $\Delta\nu = {}^1J_{^1H^{15}N}$ of the Larmor frequency of the jumping proton in the case of fast exchange are necessary; these quantities are obtained by simulation of the outer signal components of the ^1H–^{15}N signal. Note that W_0 contains, in principle, a term arising from intermolecular proton exchange; during this process a proton does not jump between the same two ^{15}N atoms but always between different ^{15}N atoms. Since the probability of a change of the spin state of the neighboring ^{15}N atom during one intermolecular exchange process is only $^1/_2$, the proton Larmor frequency is changed from $\nu + {}^1J_{^1H^{15}N}/2$ to $\nu - {}^1J_{^1H^{15}N}/2$ every other intermolecular proton exchange process. If these processes were fast all components of the ^1H–^{15}N signal would broaden and coalesce into one single line. In fact, we observed this effect when the samples were not carefully prepared. Thus, we conclude that the rate constants obtained here do not contain terms due to intermolecular proton exchange but do arise exclusively from an intramolecular double proton transfer according to Figure 1.

Finally, we ask whether there is an effect of deuteration in the NH sites on the ^1H NMR line shapes of the signal of the residual ^1H–^{15}N units of Ic. These units stem dominantly from the species Ic-HD, and only to a minor degree from the species Ic-H_2. In Figure 8 the superposed experimental and calculated spectra of Ic dissolved in $C_2D_2Cl_4$ are shown at a deuterium fraction of $D = 0.92$ in the NH sites. Naturally, it was much more difficult to obtain these spectra because of the low concentration of the residual ^1H–^{15}N units, and the experiments were, therefore, carried out at 300.13 MHz. A comparison of the spectra in Figure 7 and 8 shows that the exchange in Ic-HD is slower than in Ic-H_2. Thus, the full kinetic HH/HD/DD isotope effects could be obtained by a combination of experiments according to Figure 4–8.

^1H NMR Polarization Transfer Experiments in the Rotating Frame. As in the case of the ^{13}C NMR experiments, line shape analysis of the ^1H–^{15}N signal of Ic is not very accurate in the slow-exchange regime where the components of the exchanging and the non-exchanging lines cannot be easily separated.

Table I. Static and Dynamic Parameters of the NMR Experiments on Azophenine in $C_2D_2Cl_4$

T/K	D	method[a]	k^{HH}/s^{-1}	k^{HD}/s^{-1}	k^{DD}/s^{-1}	$\Delta\nu$/Hz	ν_1/ppm	ν_2/ppm	W_o/Hz
281	0	1	270			89.8	8.25		3.2
283	0	1	320			89.8	8.25		2.5
284.5	0	1	380			89.8	8.25		3.2
290	0	1	500			89.9	8.25		3.5
306	0	1	1500			89.8	8.25		2.0
307.5	0	1	1720			89.8	8.25		3.5
315	0	1	2800			89.7	8.25		2.7
322.5	0	1	3950			89.8	8.25		3.3
329	0	1	6000			89.8	8.25		3.4
333.5	0	1	8600			89.8	8.25		2.7
337	0	1	9000			89.6	8.25		3.5
342.5	0	1	11800			89.6	8.25		3.3
249	0	5	13.5			89.8	8.25		2.44[d]
253	0	5	32.4			89.8	8.25		3.97[d]
254.5	0	5	45.5			89.8	8.25		3.97[d]
289.4	0.92	2	930[e]	200		89.6	8.25		3.0
303.4	0.92	2	1290[e]	340		89.6	8.25		3.2
312.5	0.92	2	2290[e]	650		89.5	8.25		3.6
319.9	0.92	2	3550[e]	1050		89.6	8.25		4.0
325.2	0.92	2	4815[e]	1400		89.5	8.25		3.6
330.0	0.92	2	6280[e]	2000		89.6	8.25		3.5
338.7	0.92	2	9970[e]	3000		89.6	8.25		4.5
345.0	0.92	2	13740[e]	4700		89.6	8.25		4.0
352.0	0.92	2	19355[e]	6100		89.5	8.25		3.6
253	0	3	28			79.7[b]	124.54	123.48	3.6
263.2	0	3	64			77.8[b]	124.52	123.49	4.0
267.5	0	3	73			77.4[b]	124.49	123.47	3.7
278	0	3	230			75.4[b]	124.50	123.50	3.6
283	0	3	290			75.2[c]	124.46	123.46	3.9
250	0	4	17.3			80.0[c]			12.7[d]
283.2	0.99	3			58	75.4[b]	124.45	123.45	4.0
284.5	0.99	3			64	74.9[b]	124.43	123.45	4.0
290.0	0.99	3			104	74.5[b]	124.44	123.44	3.7
292.0	0.99	3			110	74.1[b]	124.43	123.45	3.8
299.5	0.99	3			195	73.0[c]	124.42	123.45	3.8
304.3	0.99	3			244	72.3[c]	124.38	123.42	3.7
306.0	0.99	3			295	71.9[c]	124.39	123.44	3.8
315.0	0.99	3			528	70.8[c]	124.36	123.42	4.1
319.5	0.99	3			628	70.2[c]	124.35	123.42	3.9
325.0	0.99	3			1035	69.7[c]	124.33	123.41	3.7
328.0	0.99	3			1255	68.9[c]	124.33	123.40	3.6
334.0	0.99	3			1885	68.0[c]	124.31	123.40	3.6
263.0	0.99	4			7.5				10.75[d]
265.0	0.99	4			7.3				7.7[d]

[a] Method 1: ^1H NMR line shape analysis of the ^1H–^{15}N signal of Ic at 90.02 MHz; $\Delta\nu = {}^1J_{^1H^{15}N}$. Method 2: experiments at 300.13 MHz, otherwise as with method 1. Method 3: ^{13}C NMR line shape analysis of Ia at 75.47 MHz. Method 4: ^{13}C NMR polarization transfer experiments on Ia in the rotating frame at 75.47 MHz. Method 5: ^1H NMR polarization transfer experiments on the ^1H–^{15}N signal of Ic in the rotating frame at 90.02 MHz; $\Delta\nu = {}^1J_{^1H^{15}N}$. [b] Obtained by spectral simulation. [c] Calculated according to eq 6. [d] $1/T_{1\rho}$. [e] Calculated according to eq 14.

Therefore, we also performed ^1H NMR polarization transfer experiments in the rotating frame on the ^1H–^{15}N doublet. However, by contrast to Figure 6, the polarization decays of both doublet lines I_1 and I_2 during experiment II are not exponential and are given by

$$I_i = I(0)_i\,[\exp(-t/T_{1\rho}) + \exp-(1/T_{1\rho} + 2k)t]/2, \qquad i = I_1(0) = -I_2(0) \quad (13)$$

The first term corresponds to the nonexchanging part of each doublet line, the second term to the exchanging part. Thus, $T_{1\rho}$ and k can be obtained from experiment II alone. Note that even in the absence of exchange $T_{1\rho}$ is different in experiment I and II;[68] from this difference information can be obtained on the ^1H–^{15}N bond length and the correlation time of the molecular motion. Actually, we found an ^1H–^{15}N bond length of 105 ± 9 pm, and a correlation time of τ = 1.6 ± 0.9 ns at 254.5 K, assuming an isotropic reorientation of the ^1H–^{15}N vector. Since these experiments are beyond the scope of this study they will be described elsewhere.

Kinetic HH/HD/DD Isotope Effects of the Tautomerism of Azophenine in $C_2D_2Cl_4$. As mentioned above, the full kinetic HH/HD/DD isotope effects of the reaction of AP in $C_2D_2Cl_4$ were obtained by a combination of the different NMR experiments described above, neglecting heavy-atom isotope effects on the reaction. The results of all experiments are assembled in Table I. The actual experiments were done in the following order. First,

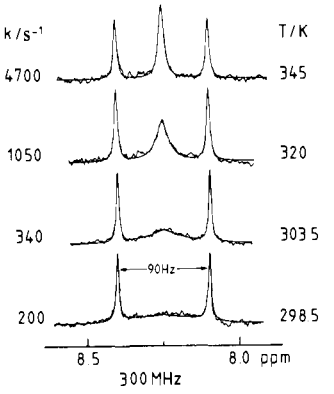

Figure 8. Superposed experimental and calculated 300.13-MHz ^1H NMR signals of the ^1H–^{15}N units of Ic dissolved in $C_2D_2Cl_4$. Deuterium fraction in the NH sites, D = 0.92. A total of 1000–5000 scans, 90° pulses, 4-s repetition time.

(68) Goldman, M. *J. Magn. Reson.* **1984**, *60*, 437.
(69) Martin, G. J.; Martin, M. L.; Gouesnard, J. P. *^{15}N-NMR Spectroscopy, NMR Basic Principles and Progress*; Springer: Berlin, 1981; Vol. 18.

Table II. Static and Dynamic Parameters of the ^1H NMR Experiments on Ic in Different Solvents[a]

T/K	D	method	solvent	k^{HH}/s^{-1}	$\Delta\nu$/Hz	δ/ppm	W_0/Hz
281.0	0	2	2	300	89.8	8.45	3.3
290.0	0	2	2	510	89.8	8.45	3.3
297.0	0	2	2	720	89.8	8.45	3.3
304.0	0	2	2	1200	89.8	8.45	3.2
312.2	0	2	2	2000	89.8	8.45	3.4
318.3	0	2	2	2850	89.8	8.45	3.2
326.2	0	2	2	4450	89.8	8.45	3.3
335.2	0	2	2	7000	89.8	8.45	3.2
342.0	0	2	2	9100	89.8	8.45	3.0
282.9	0	1	3	300	89.8	8.25	2.9
291.0	0	1	3	550	89.8	8.25	2.9
313.3	0	1	3	2500	89.8	8.25	2.8
320.4	0	1	3	3260	89.8	8.25	2.6
327.2	0	1	3	5000	89.8	8.25	2.6
345.3	0	1	3	9800	89.8	8.25	2.6
287.5	0	1	4	330	89.8	8.5	1.9
292.9	0	1	4	380	89.8	8.5	2.0
297.5	0	1	4	710	89.8	8.5	2.9
309.0	0	1	4	1200	89.8	8.4	2.8
315.0	0	1	4	1800	89.8	8.4	2.3
326.0	0	1	4	3400	89.8	8.4	3.1
342.5	0	1	4	9000	89.8	8.5	3.0
313.0	0	1	5	1800	89.8	8.6	3.0
340.0	0	1	5	6000	89.8	8.6	3.2
330.5	0	1	5	5000	89.8	8.6	4.1
303.0	0	2	6	850	89.8	8.5	2.0

[a] Methods as in Table I. Solvent 1, $C_2D_2Cl_4$; solvent 3, 1,2-dichloroethan-d_4; solvent 4, tetrahydrofuran-d_8; solvent 5, toluene-d_8; solvent 6, benzonitrile-d_5. All other parameters as described in the text.

we performed the line shape analysis of the ^1H–^{15}N NMR signal of Ic in $C_2D_2Cl_4$, as shown in Figure 6, from which the rate constants k^{HH} were obtained. For comparison, some experiments were also performed on Ia, but the k^{HH} values were the same within the margin of error. These measurements of k^{HH} were completed by low temperature polarization transfer experiments of Ic. Since W_0 and the frequency difference $\Delta\nu$ between the exchanging lines are known from the nonexchanging components of the ^1H–^{15}N signal, and since in the polarization transfer experiments the exchange rates are directly measured, the values for k^{HH} listed in Table I are free from systematic errors that could arise from assumptions concerning W_0 or $\Delta\nu$.

In order to obtain the rate constants k^{HD} we then performed ^1H NMR measurements on Ic in $C_2D_2Cl_4$ at a deuterium fraction $D = 0.92$, as shown in Figure 7. Although Ic-D_2 is the dominant species, it does not contribute to the ^1H–^{15}N signal. The fraction of the signal intensity corresponding to the species Ic-HD is equal to the deuterium fraction D; a minor fraction $1 - D$ stems from residual Ic-H_2. In order to take into account the presence of the latter, the computer program was modified in the sense that the presence of two types of $^{15}NH\cdots{}^{15}N$ hydrogen-bonded systems were allowed, one characterized by the population D and the rate constant k^{HD} and the other by the population $1 - D$ and the rate constants and k^{HH}; the exchange problem was the same for both types. Since D and k^{HH} were known, only k^{HD} was varied in the simulations shown in Figure 7. Thus, k^{HD} could also be obtained without assumptions. Polarization transfer experiments on Ic-HD could not be carried out because of its low concentration and the resulting bad signal-to-noise ratio. We then evaluated the kinetic data obtained in the ^{13}C NMR experiments. First, we compared the values of k^{HH} obtained by ^1H and ^{13}C NMR polarization transfer experiments. They agreed very well, indicating that both methods monitor the same dynamic process. In fact, we then took the k^{HH} values obtained by ^1H NMR as fixed entries into the ^{13}C line shape calculations at $D = 0$, and only the line width W_0 in the absence of exchange was varied. $\Delta\nu$ was obtained as described in Figure 5, by simulation of the spectra at $D = 0$ and $D = 0.99$. As shown in Table I, the W_0 values are quite large and are most probably affected by short intrinsic T_2 processes and only to a small extent by apparative line broadening such as the inhomogeneity of the magnetic field and a residual broadening from ^1H decoupling. This interpretation is confirmed by the observation of quite small $T_{1\rho}$ values, which are approximately equal to the T_2 values.

We came then to the last stage of the measurements, i.e., the evaluation of the rate constants k^{DD} from ^{13}C NMR experiments at a deuterium fraction of $D = 0.99$. The most direct measurement of k^{DD} was obtained by the polarization transfer method according to Figure 6 in the low-temperature region. Since W_0 was known from the simulations at $D = 0$, we could obtain, especially in the region of the coalescence, k^{DD} values that do not suffer from approximations.

The kinetic data of the tautomerism of azophenine in $C_2D_2Cl_4$ can now be summarized as follows:

$$k^{HH} = 10^{11.62\pm0.14} \exp(-49.42 \pm 0.75 \text{ kJ mol}^{-1}/RT), \quad 249 \le T \le 343 \text{ K} \quad (14)$$

$$k^{HD} = 10^{11.94\pm0.17} \exp(-54.7 \pm 0.9 \text{ kJ mol}^{-1}/RT), \quad 298 \le T \le 352 \text{ K} \quad (15)$$

$$k^{DD} = 10^{12.05\pm0.25} \exp(-56.2 \pm 1.4 \text{ kJ mol}^{-1}/RT), \quad 263 \le T \le 334 \text{ K} \quad (16)$$

with the kinetic isotope effects

$$k^{HH}/k^{HD} = 4.1,\ k^{HD}/k^{DD} = 1.4, \text{ i.e., } k^{HH}/k^{DD} = 5.6 \quad (17)$$

at 298 K.

Solvent Effects on the Tautomerism of Azophenine. In order to probe a possible solvent effect on the tautomerism of AP we performed additional ^1H NMR experiments of Ic in various solvents. In all cases, the spectral behavior followed the pattern shown in Figure 7. The results are given in Tables II and III. Although the dielectric constant was varied between 2.4 and 25, the rate constants k^{HH} were almost independent of the type of solvent used.

^{15}N CPMAS NMR Study of Solid-State Effects on the Tautomerism of Azophenine. In order to know whether the tautomerism of AP also takes place in the solid state we performed ^{15}N NMR experiments on Ib under the conditions of cross polarization (CP) and magic angle spinning (MAS). The spectra are shown in Figure 9. As expected,[15-17,19-22] we observe at low temperatures a high-field ^{15}N line, characteristic for the NH sites, and a low-field line, characteristic for the =N— sites. As the temperature is raised from 200 to 300 K no change in the line splitting $\Delta\nu$ is observed, indicating slow proton exchange, as expected from the liquid NMR studies. The situation resembles the one shown in the lower spectrum of Figure 3. However, as the temperature is raised further from 300 to 400 K, the two lines suddenly move toward each other, the low-field shift of the high-field line matching the high-field shift of the low-field line. The shifts are listed in Table IV. This situation is understandable in terms of the upper spectrum in Figure 3b with the presence of two very unequally populated tautomers which interconvert fast above 300 K. Using eq 5, one can calculate the equilibrium constant K_{12}

Table III. Kinetic Parameters of the Double Proton Transfer in Azophenine in Different Solvents

solvent	DK	E_a/kJ mol^{-1}	A/s^{-1}	k^{HH}_{303K}	T range/K
toluene-d_8	2.4			1000	
chloroform-d_1	4.8	45.9 ± 0.75	10.98 ± 0.14	1170	281 ≤ T ≤ 342
tetrahydrofuran-d_8	7.6	47.5 ± 2.5	11.1 ± 0.3	823	287 ≤ T ≤ 342
1,1,2,2-tetrachloroethane-d_2	8.2	49.42 ± 0.75	11.62 ± 0.14	1260	249 ≤ T ≤ 343
1,2-dichloroethane-d_4	10.4	47.5 ± 2.5	11.04 ± 0.3	1190	283 ≤ T ≤ 345
benzonitrile-d_5	25			950	

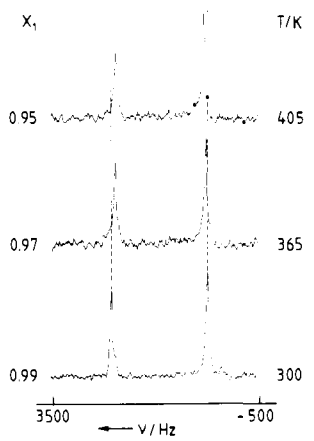

Figure 9. The 9.12-MHz solid-state ^{15}N CPMAS NMR spectra of Ib as a function of temperature. A 2-kHz sample rotation, 20 000–30 000 scans on average, 1.2 ms CP time, 2.5-s repetition time, reference $(^{15}NH_4)_2SO_4$.

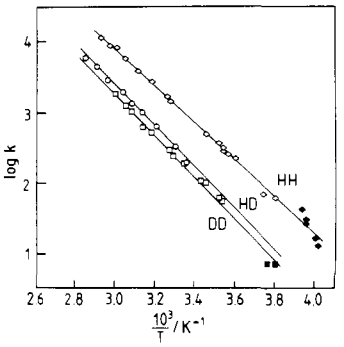

Figure 10. Arrhenius diagram of the HH, HD, and the DD transfer in I dissolved in $C_2D_2Cl_4$.

Table IV. Equilibrium Constants K_{12} of the Solid-State Tautomerism of AP Obtained by ^{15}N CPMAS NMR Spectroscopy of Crystalline Ib[a]

T/K	$\delta\nu$/Hz	K_{12}
223	1860	
250	1860	
300	1860	
340	1780	0.022
365	1740	0.032
405	1690	0.046

[a] All parameters are described in the text.

of tautomerism from the ratio between the observed reduced high-temperature splitting $\delta\nu$ and the low-temperature splitting $\Delta\nu$. These constants are very small and are listed in Table 4. From a plot of log K_{12} vs $1/T$ we calculate the reaction enthalpy and entropy of

$$\Delta H_{12} = 12 \pm 2 \text{ kJ mol}^{-1}$$
$$\text{and } \Delta S_{12} = 0.4 \pm 0.4 \approx 0 \text{ J K}^{-1} \text{ mol}^{-1} \quad (18)$$

Thus, there is a solid-state effect in the sense that the degeneracy of the two tautomers in Figure 1 is lifted. The proton transfer itself is, however, not suppressed in the crystalline state, although very slow at low temperatures. Because of the very small fraction of the second tautomer, dynamic NMR line broadening, as expected in the middle spectrum of Figure 3b, is smaller than the overall line widths and could not be detected in this study.

Discussion

By use of different methods of dynamic NMR spectroscopy, the tautomerism of azophenine (AP; Figure 1) has been studied as a function of the environment, isotopic H/D substitution in the NH sites, and temperature. In this section we will discuss what can be learned about the proton dynamics in AP from these experiments. Let us, for this purpose, summarize the main experimental results.

When the molecule is dissolved in a liquid, the protons move along apparently symmetric double minimum potentials with two degenerate tautomeric states, as expressed by Figure 1. Not shown in Figure 1 are the nuclear spin functions, which label the molecule in such a way that the two states are no longer related by symmetry but interconvert only via double proton transfer. This makes the two states at low temperatures distinguishable by NMR. At higher temperatures, line shape changes are observed that allowed us to determine the rate constants of the double proton transfer. They follow an Arrhenius law and are independent of the type of the solvent whose dielectric constant was varied between 2 (toluene) and 25 (benzonitrile). Full kinetic HH/HD/DD isotope effects were obtained for tetrachloroethane as a solvent. The kinetic HH/HD isotope effect of tautomerism in AP is substantially greater than the kinetic HD/DD isotope effect, indicating a breakdown of the rule of the geometric mean for the AP tautomerism. In addition, the overall kinetic HH/DD isotope effects were smaller as compared to previous double proton transfer systems. Further NMR measurements show that the double proton transfer in AP is not suppressed in the solid state. However, the liquid solution degeneracy of the two tautomeric states is lifted in the solid; in the latter the protons move, therefore, along a strongly asymmetric reaction energy surface. We should also mention that recent liquid- and solid-state IR experiments on AP indicate a coupling of the two NH oscillators.[58]

In the discussion of the reaction mechanism we first address the problem of inter- vs intramolecular hydrogen bonding and proton transfer in AP. Then the question arises whether the kinetic results support a tunnel mechanism from excited vibrational states. We then come to the problem of whether the motion of the two protons in AP is coupled or not. Before this question is discussed in relation to the observed kinetic isotope and solvent effects, we will specify the different degrees of coupling encountered when two proton transfer systems are brought into contact with each other. The observed liquid- and solid-state effects on the AP tautomerism will be interpreted in terms of a "static" solvent effect, by which the microscopic double minimum potentials of symmetric reactions like the AP tautomerism are affected in ordered or disordered environments. Finally, the nature of these distortions is discussed.

Intra- vs Intermolecular Hydrogen Bonding and Double Proton Transfer in Azophenine. The temperature-dependent NMR signals of the labile ^1H–^{15}N protons of AP are direct proof that the observed tautomerism proceeds via an intra- and not via a possible intermolecular pathway. At low temperatures these signals are split into a ^1H–^{15}N doublet (Figures 7 and 8) because the H-bond proton experiences only one ^{15}N atom as neighbor. The observed triplet splitting at high temperatures indicates then that the labile proton jump rapidly between always the same two ^{15}N atoms, which is typical for an intramolecular process. By contrast, intermolecular proton exchange would lead to a collapse of the ^1H–^{15}N doublet into a singlet.[6,10,14] Thus, the rate constants obtained here do not contain terms due to the latter process.

The question of whether and how the NH protons and AP are involved in hydrogen bonding is less easily answered. Since the ^1H chemical shifts of the ^1H–^{15}N protons are remarkably independent of the concentration, temperature, and solvent, one can exclude the formation of intermolecular hydrogen bonds by AP. Thus, if the NH protons of AP form hydrogen bonds, the latter must be intramolecular, as shown in Figure 1. These hydrogen bonds cannot be very strong in view of the observation that the NH stretching band of AP is not particularly shifted to low frequencies ($\approx$3300 cm^{-1});[58] however, the band is quite intense, as expected for a weak NH···N bond. This conclusion is supported by the observation that the chemical shift of the NH protons in AP is of the order of 8–9 ppm, depending on the solvent; this value is smaller than that in the strongly intermolecularly hydrogen-bonded reference compound Ph-NHCH=CHCH=N-Ph molecule, where the NH chemical shifts are of the order of 11–12 ppm.[10] Also, the ^1H–^{15}N distance of $\sim$105 pm found here from

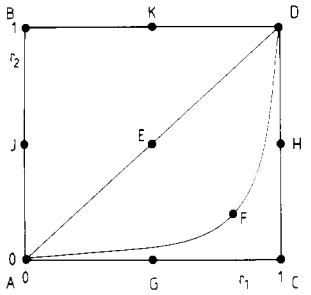

Figure 11. Double proton transfer pathways. Key: A, initial state; D, final state; B, C, and E–G, possible intermediate nuclear configurations; r_i, relative displacement of proton i.

longitudinal relaxation experiments in the rotating frame is consistent with the formation of weak NH···N hydrogen bonds which facilitate the intramolecular double proton transfer.

Does the Azophenine Tautomerism Proceed by Vibrationally Activated Tunneling? Let us now discuss the question of whether the double proton transfer in AP proceeds by thermally activated tunneling from excited vibrational levels, for example, the NH stretching levels, as has been proposed for different reasons by us[3] and by Dewar et al.[52] The kinetic measurements carried out here provide no strong evidence for such a process. For unimolecular over-barrier reactions characterized by activation entropies of the order of zero, transition-state theory predicts preexponential factors of the Arrhenius equation of the order of 10^{13} s^{-1}. Some tunneling theories[3,45,47] use the frequencies of AH stretching vibrations as reference value, which are of the order of 10^{14} s^{-1}. According to Bell, smaller values are expected if proton tunneling is involved in the reaction and if the experimentally accessible temperature range is limited.[47] As indicated in eq 14–16, we find here for the AP tautomerism preexponential factors of the order of 10^{12} s^{-1}. This means that if thermally activated proton tunneling is involved it must proceed from vibrational levels that are located not far below the top of the barrier. Therefore, it seems unlikely that the difference between the experimental energies of activation found here for AP and the barrier heights calculated by Dewar et al.[52] for 11, using the AM1 method, can be attributed to tunneling from excited vibrational levels located well below the top of the barrier. If this difference does not arise from the approximations inherent in the calculations, it must come either from the presence of the phenyl groups in AP, from solute–solvent interactions, or from the possibility that the true transition state has not yet been theoretically found.

Nevertheless, it is interesting to discuss the location of the excited NH stretching states of AP with respect to the experimental barrier for the proton transfer, which is of the order of 3500 cm^{-1} as can be calculated from eq 14. Since the NH stretching frequency is of the order of 3300 cm^{-1}, the first excited NH stretching states must lie just below the top of the barrier. By contrast, the second excited stretching states ($\sim$6400 cm^{-1}), which have been observed recently,[58] are then located well above the barrier of proton transfer. The fact that there is only a very small anharmonicity associated with the corresponding overtone stretching bands seems to indicate that the proton transfer reaction coordinate is not simply equal to the normal mode of the NH stretching vibration, as was proposed previously.[3] However, the existence of these overtone bands will be important information for the quantum mechanical description of the tautomerism of polyatomic molecules.[51]

Coupling between Double Proton Transfer Systems. In order to provide a framework for the following discussion, we have to specify the different kinds of coupling that occur when two protons, located in two different proton transfer systems i = 1, 2, interact via the electron system. Let each proton i exist in two equilibrium positions characterized by the displacements r_i = 0 and 1, as shown in Figure 11. If the molecular potential energy surface is such that the forces acting on proton i depend on r_j, a coupled proton motion results. When the displacements are small, this phenomenon leads to a directly observable *vibrational coupling* of the two

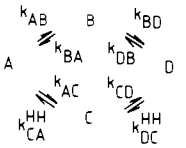

Figure 12. Single proton transfer network with the nuclear configurations A–D of Figure 11 as observable species.

stretching vibrations in which the two protons are involved.[50,58] Note that vibrational coupling is not restricted to proton transfer systems but occurs in any molecular system. When the displacements become larger during the course of the proton transfer between different potential wells, a *kinetic coupling* of the proton motion can occur. Finally, we must also discuss a *thermodynamic coupling of the two proton transfer systems.* In view of the scope of this study, this section is essentially devoted to a discussion of the latter two types of coupling.

Let us first discuss the case where all possible nuclear configurations A (r_1 = 0, r_2 = 0), B (r_1 = 0, r_2 = 1), C (r_1 = 1, r_2 = 0), and D (r_1 = 1, r_2 = 1) in Figure 11 correspond to observable species, i.e., to minima in the two-dimensional energy surface which interconvert via *single proton transfers*. This situation can be described in terms of the reaction network shown in Figure 12, characterized by three independent equilibrium constants

$$K_{nm} = C_m/C_n = k_{nm}/k_{mn} \quad m, n = A–D$$

where C_m is the concentration of state m and k_{mn} the rate constant between states m and n. It is now useful to define the proton density ratios

$$K_1 = C\{r_1 = 1\}/C\{r_1 = 0\} = (C_B + C_D)/(C_A + C_C) \tag{19}$$

and

$$K_2 = C\{r_2 = 1\}/C\{r_2 = 0\} = (C_C + C_D)/(C_A + C_B) \tag{20}$$

By simple arithmetic it follows that[19,21]

$$K_1 = K_{AB}(1 + K_{BD})/(1 + K_{AC}) \tag{21}$$

and that

$$K_2 = K_{AC}(1 + K_{CD})/(1 + K_{AB}) \tag{22}$$

Equations 21 and 22 can be used to define the degree of *thermodynamic coupling* of the two *single proton transfer systems* i,j = 1, 2. These systems are said to be *thermodynamically decoupled* if

$$\begin{aligned} &K_{AB} = K_{CD} \text{ and } K_{AC} = K_{BD}, \\ &\text{i.e., } K_1 = K_{AB} \text{ and } K_2 = K_{AC} \end{aligned} \tag{23}$$

This means that the proton transfer equilibrium i does not depend on the state of the proton transfer system j, i.e., only two equilibrium constants are needed according to eq 23 for the description of the reaction network. The latter splits up in two independent single proton transfer reactions. In other words, r_1 and r_2 in Figure 11 behave like normal coordinates. This case is realized per definition if the two protons are located, for example, in different molecules which may be far apart from each other.

If the proton transfer systems are located close to each other, a *thermodynamic coupling* of the two proton transfer systems occurs in the sense that the equilibrium of proton i becomes dependent on the state of proton j. Then, eq 23 does not hold any more, i.e., $K_{AB} \neq K_{CD}$ and $K_{AB} \neq K_{BD}$. Actually, K_{AB} and K_{AC} decrease, whereas K_{BD} and K_{CD} increase. However, all states A–D are still observable. As the thermodynamic coupling increases the concentrations of states B and C will, however, decrease, which renders the direct spectroscopic observation of B and C impossible. B and C may then be regarded as intermediates of the *double proton transfer reaction* A → B → D or A → C → D, which still consists of two consecutive single proton transfer reactions. It can easily be shown that the observed rate constant k_{AD} is given by

$$k_{AD} = \frac{k_{AB}k_{BD}}{k_{BA} + k_{BD}} + \frac{k_{AC}k_{CD}}{k_{CA} + k_{CD}} \tag{24}$$

As K_{AB}, K_{AC}, K_{BD}^{-1}, and K_{CD}^{-1} become zero, the intermediates C and D become transition states of the double proton transfer between the initial state A and the final state D. It then follows from eqs 21 and 22 that

$$K_1 \approx K_{AB}K_{BD} \equiv K_{AD} \text{ and } K_2 \approx K_{AC}K_{CD} \equiv K_{AD}, \quad \text{i.e. } K_1 = K_2 \tag{25}$$

Thus, the reaction network in Figure 12 collapses into one single double proton transfer reaction characterized by a single equilibrium constant. In other words, eq 25 represents the theoretical borderline between a *stepwise transfer* of two protons in two thermodynamically coupled single proton transfer systems and a *kinetically coupled motion of two protons in a double proton transfer system*. The latter process can take place along different pathways, of which the following two are to be regarded as extremes. The pathway A → E → D corresponds to a *synchronous* motion because $r_1 = r_2$ at all stages of the reaction. By contrast, the pathways A → B → D and A → C → D where B and C are transition states rather than intermediates can be called *asynchronous*. Note that from an experimental standpoint it is useful to introduce the term "*correlated*" double proton transfer when only the states A and D can be observed experimentally. This notion leaves the question open as to whether the proton motion is kinetically coupled or stepwise.

For convenience, let us summarize the different notions introduced in this section. A *vibrationally coupled proton motion* can already occur in the potential wells. During a *kinetically* coupled double proton transfer across the barrier, both protons are more (*synchronous motion*) or less (*asynchronous* motion) in flight in the transition state. This case cannot be easily distinguished experimentally from a *stepwise process* in which intermediates formed by *kinetically decoupled* single proton transfers are not directly observable. In both cases the proton motion is, therefore, called *correlated* because only two tautomers are observed which interconvert by the transfer of both protons. Direct evidence for a kinetically decoupled proton motion is obtained when the intermediate tautomers become spectroscopically observable species. As long as the equilibrium in the proton transfer system *i* depends on the state of the proton transfer system *j* we call the two systems *thermodynamically coupled*.

Vibrational Coupling of the Two NH Oscillators in Azophenine. Evidence for a vibrational coupling of the two NH oscillators in AP comes from IR experiments performed on this molecule in the crystalline state.[58] It was found that the NH stretching frequency of AP-HD is shifted to higher wavenumbers as compared to the main stretching band of AP-H_2. This observation means that when one NH bond is stretched a force arises that shortens the second NH bond. A similar observation was made previously for the two NH oscillators of *meso*-tetraphenylporphine[50] where, however, the two NH units are spatially very close to each other. In the case of AP, the two NH units are far from each other and they must communicate via the electronic system. Although these IR experiments do not tell us what happens during the reaction, they indicate that the forces acting on one proton depend on the location of the second proton.

Pathways of the Azophenine Tautomerism. Let us specify now the general reaction network of Figure 11 for the case of the tautomerism of AP as shown in Figure 13. The two observed tautomers of Figure 1 correspond to points A and D in Figures 11 and 13. Since no additional tautomers can be detected spectroscopically, eq 24 is fulfilled at least experimentally, i.e., the double proton transfer in AP is *correlated*. We do not yet know, however, whether the transfer is kinetically coupled or whether it occurs stepwise via intermediates. Thus, we have to discuss the different proton transfer pathways illustrated in Figure 13, which involve transition states with either two, zero, or one protons in flight. Pathways a and b represent the two extremes of the kinetically coupled proton motion. Pathway a involves a synchronous motion of the two protons via the transition state E. By contrast, pathway b involves an asynchronous proton motion via the transition state B or C, in which no proton is in flight. Pathway c corresponds to the case of the stepwise motion of two

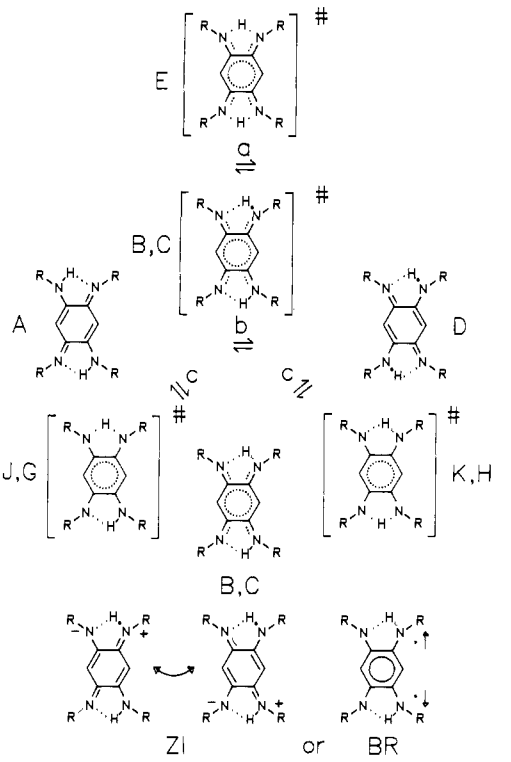

Figure 13. Double proton transfer pathways of azophenine. The capital letters correspond to the nuclear configurations in Figure 11.

protons in two thermodynamically strongly coupled single proton transfer systems, involving two consecutive single proton transfers with B or C as intermediates. G, J and K, H are the corresponding transition states with single protons in flight. As shown at the bottom of Figure 13, one can imagine different resonance structures for B (and for C), i.e., highly polar zwitterionic structures ZI and an apolar singlet biradical structure BR in which all electrons remain spin-paired. It is also conceivable that ZI and BR are not resonance structures for the same nuclear configuration but that they have different geometries corresponding to different minima in the energy potential surface. Note that depending on the electronic nature of B and C the transition states G–K are either polar or apolar.

Theoretical evidence for pathway c involving the zwitterionic intermediate comes from semiempirical calculations performed by Dewar et al.[52] on II (Figure 1), whereas the cyclic transition state E in pathway a was found to correspond to a hilltop in the potential surface rather than to a saddle point. We will discuss now whether our kinetic results contain information concerning the proton transfer pathways. We first discuss the kinetic HH/HD/DD isotope and then the solvent effects.

Kinetic HH/HD/DD Isotope Effects and Breakdown of the Rule of the Geometric Mean. The fact that the AP tautomerism involves a kinetic isotope effect of $k^{HH}/k^{DD} = 5.6$ at 298 K indicates that it is indeed the proton transfer that is the rate-limiting step of the reaction. This value is significantly smaller than the corresponding values found previously for the double proton transfer between acetic acid and methanol[3,13] and for the porphine tautomerism.[3] By contrast, we also find here for AP a substantial deviation from the rule of the geometric mean (RGM) because $k^{HH}/k^{HD} = 4.1$ and $k^{HD}/k^{DD} = 1.4$ at 298 K. How have these results to be interpreted?

In principle, if it were possible to calculate rate constants including kinetic isotope and solvent effects for a given pathway on a purely quantum mechanical basis one could obtain information about the real pathway by comparison with the experimental kinetic data. Unfortunately, it has so far not been possible to perform such calculations because of the multidimensional character of even simple reactions like the tautomerism of AP. The following considerations are, therefore, based on a conven-

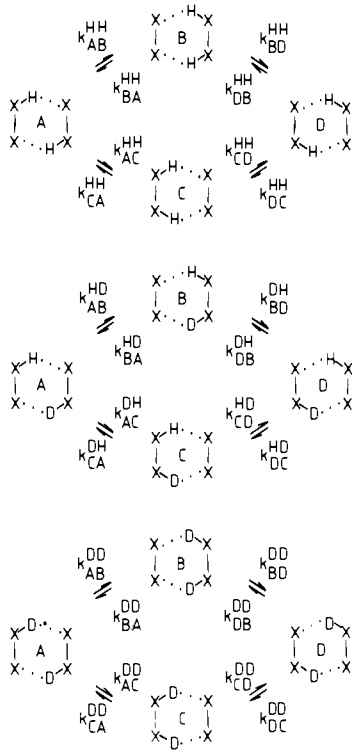

Figure 14. Isotopic exchange reactions in a general stepwise double proton transfer reaction.

tional semiclassical treatment of kinetic isotope effects rather than on an exact theory.

Theoretical calculations within the framework of transition-state theory (TST) have shown that for the synchronous pathway A → E → D, i.e., for the AP pathway a in Figure 13, the RGM should hold in good approximation.[3,43,44] Therefore, our observation of the breakdown of the RGM does not support this pathway. Note, however, that this pathway cannot be excluded completely because the contribution of tunneling could also lead to a partial breakdown of the RGM,[3,13] even in the case of a synchronous proton motion. In addition, it does not seem impossible that a full quantum mechanical treatment could explain the observed breakdown of the RGM even if no tunneling is involved, i.e., if the reaction proceeds from certain vibrational levels that are located above the barrier of proton transfer and that are different for AP-H_2, AP-HD, and AP-DD.

The situation is similar for the transition state of the reaction pathway b in Figure 13, i.e., for an asynchronous proton motion. In terms of TST it is easy to show that the zero-point energy of the AP-HD transition state must be given approximately by the arithmetic mean of the corresponding zero-point energies of the HH and the DD transition states. Therefore, according to arguments given previously,[3] the RGM should also hold for pathway b, which is, consequently, not considered further.

We ask then whether our kinetic data support a stepwise proton motion according to pathway c in Figure 13. In order to evaluate the kinetic isotope effects for this pathway, we have to consider the different isotopic reactions shown for a general stepwise double proton transfer reaction in Figure 14. Note that in the case of AP the educt A and the product D are equivalent; the same is true for the intermediates B and C. The different rate constants in Figure 14 have the form $k_{ij}^{L_1L_2}$, L_1,L_2 = H or D. L_1 characterizes the hydrogen isotope transferred during the step $i \rightarrow j$ and L_2 the isotope in the site that is nonreactive during this step. Since for AP the states A and D as well as B and C in Figure 15 are equivalent, it follows that

$$k_{AB}^{L_1L_2} = k_{AC}^{L_1L_2} = k_{DB}^{L_1L_2} = k_{DC}^{L_1L_2} \text{ and } k_{BA}^{L_1L_2} = k_{CA}^{L_1L_2} = k_{BD}^{L_1L_2} = k_{CD}^{L_1L_2} \quad (26)$$

Therefore,

$$k_{AB}^{HD}/k_{BA}^{HD} = k_{AC}^{DH}/k_{CA}^{DH} = k_{AB}^{DH}/k_{BA}^{DH} \quad (27)$$

By combination of eq 24, 26, and 27, we then obtain

$$k_{AD}^{HH} = k_{AB}^{HH},\ k_{AD}^{DD} = k_{AB}^{DD}, \text{ and } k_{AD}^{HD} = k_{AD}^{DH} = 2[k_{AB}^{HD}\,k_{BA}^{DH}/(k_{BA}^{HD} + k_{AB}^{DH})] \quad (28)$$

It is then useful to define the primary

$$P_{ij}^{H} = k_{ij}^{HH}/k_{ij}^{DH},\ P_{ij}^{D} = k_{ij}^{HD}/k_{ij}^{DD} \quad (29)$$

and the secondary

$$S_{ij}^{H} = k_{ij}^{HH}/k_{ij}^{HD},\ S_{ij}^{D} = k_{ij}^{DH}/k_{ij}^{DD} \quad (30)$$

kinetic isotope effects of the step $i \rightarrow j$. By introducing eq 29 and 30 into eq 28 and writing $k_{AD} \equiv k$, it follows that

$$\frac{k^{HD}}{k^{HH}} = \frac{2(S_{AB}^{H}P_{AB}^{H})^{-1}}{(S_{AB}^{H})^{-1} + (P_{AB}^{H})^{-1}} \text{ and } \frac{k^{HH}}{k^{DD}} = S_{AB}^{D}P_{AB}^{H} = P_{AB}^{D}S_{AB}^{H} \quad (31)$$

Since secondary isotope effects are, generally, small the following equation

$$S_{AB}^{H} = S_{AB}^{D} = S_{AB} = S, \text{ i.e., } P_{AB}^{H} = P_{AB}^{D} = P_{AB} = P \quad (32)$$

should hold in good approximation. We then obtain

$$\frac{k^{HD}}{k^{DD}} = \frac{2}{S^{-1} + P^{-1}} \text{ and } \frac{k^{HH}}{k^{DD}} = P{\cdot}S \quad (33)$$

Thus, the P and S can be calculated if the kinetic isotope effects k^{HH}/k^{DD} and k^{HD}/k^{DD} are known experimentally. For the case that $S = 1$ it follows from eq 33 that

$$k^{HD} = 2k^{DD}/(1 + k^{DD}/k^{HH}) \quad (34)$$

Equation 34 has been given previously.[3] Note that for the derivation of these relations no particular kinetic theory has been used. Therefore, eq 31–34 are valid whether the reaction proceeds over the barrier or by tunneling.

We have now calculated P and S for the AP tautomerism from the kinetic data expressed by eq 14–17 in terms of eq 33. We are able to accommodate the experimental data in terms of the following equations:

$$P = 0.47 \exp(7 \text{ kJ mol}^{-1}/RT),\ P_{298K} = 7.2 \quad (35)$$

$$S \approx 0.82 \exp(-0.3 \text{ kJ mol}^{-1}/RT) \approx 1.0 \exp(-0.6 \text{ kJ mol}^{-1}/RT),\ S_{298K} = 0.78 \quad (36)$$

Note that the calculated Arrhenius curves derived by eq 33, 35, and 36 cannot be distinguished in Figure 10 from those calculated by linear regression analysis of the experimental data, i.e., from eq 14–17. S is smaller than 1, which signifies that the secondary kinetic isotope effect is inverse. In terms of transition-state theory this means that the vibrational zero-point energy of the nonreactive hydrogen isotope increases slightly during the jump of the reactive hydrogen isotope. By contrast, the zero-point energy of the reactive hydrogen is lost in the transition state, leading to values of $P > 1$. Since $S < 1$, it follows from eq 31 that P is larger than the observed values of k^{HH}/k^{DD}. Since P refers to a single proton transfer, there is no need to invoke major heavy-atom motions to explain this value, which is in the range of values predicted by transition-state theory.[35,47] Thus, we can conclude that the kinetic HH/HD/DD isotope effects presented here can be quantitatively explained in terms of pathway c.

Dynamic Solvent Effects. It is an old experience in physical organic chemistry that the rate constants of reactions involving neutral educts and products but highly polar or ionic transition states or intermediates are especially sensitive to the dielectric constant of the solvent.[70,71] This effect arises because the polar intermediates or transition states are, generally, strongly solvated. As a consequence, the solvent molecules are highly ordered around the reacting species leading to large negative entropies of activation.[71] For certain reactions the absolute rate constants are not

(70) Reichardt, C. *Lösungsmitteleffekte in der Organischen Chemie*; Verlag Chemie: Weinheim, 1969.

(71) Gompper, R. *Angew. Chem.* **1969**, *81*, 348; *Angew. Chem., Int. Ed. Engl.* **1969**, *8*, 312.

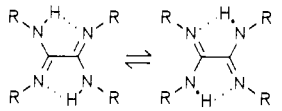

Figure 15. Tautomerism of tetraphenyloxalamidin (TPOA).

very different in different solvents because of an entropy–enthalpy compensation; however, the large negative activation entropies still indicate a strong interaction between the polar intermediates and the solvent molecules.[71] Negative activation entropies imply observed frequency factors that are much smaller than 10^{13} s^{-1}; the latter corresponds to an activation entropy of about zero.

A look at eq 14–17 and Table III shows that the observed frequency factors of the AP tautomerism are not far from 10^{13} s^{-1}, i.e., the activation entropies are close to zero and that—within the margin of error of about 10%—the reaction rates are independent of the type of solvent. Note that the reaction proceeds with the same rate in toluene (DK = 2) and in benzonitrile (DK = 25)! This finding precludes the formation of strongly solvated polar intermediates or transition states during pathway c in Figure 13. *Although pathway a involving nonclassical kinetic isotope effects cannot completely be excluded, the only remaining possibility that easily accommodates the experimental kinetic solvent as well as the kinetic isotope effects seems then to be pathway c in Figure 13, with a nonsolvated zwitterion or an apolar singlet biradical as intermediate.* Unfortunately, no theoretical calculations are available at present from which the energy of this biradical might be estimated and which might support this conclusion.

Comparison with Tetraphenyloxalamidine (TPOA). At this stage it is interesting to compare the results obtained here for the AP tautomerism with those obtained recently in this laboratory for the tautomerism of the structurally related TPOA molecule shown in Figure 15.[6] Although the TPOA molecule is subject to all kinds of conformational and intermolecular proton-exchange processes, some rate constants of the intramolecular double proton transfer could be measured by using CD_2Cl_2 as solvent with similar methods as reported here for azophenine. Surprisingly, the activation parameters for the AP and the TPOA rearrangement are almost equal to those of AP. E.g., here we find $k_{303K} \approx 1000$ s^{-1} (Tables I and II), whereas the TPOA rearrangement proceeds with a rate constant of $k_{303K} \approx 2400$.[6] Thus, in first approximation, the greater extended molecular skeleton of AP as compared to TPOA seems to have only a minor influence on the reaction rates of the tautomerism. Note, however, that we do not know whether the proton transfer pathways in both compounds are similar, because it was not possible in the case of TPOA to measure either full kinetic HH/HD/DD isotope or intrinsic kinetic solvent effects. The reason for this failure was the finding that this molecule is subject to a complicated solvent-dependent conformational reaction network, involving not only the intramolecularly hydrogen-bonded conformer shown in Figure 15 but additional conformers which form strong intermolecular hydrogen bonds.

Solid-State and Static Solvent Effects on the Azophenine Tautomerism. At first sight, the absence of dynamic solvent effects on the AP tautomerism could lead to the conclusion that this process is not influenced by intermolecular interactions. In this case, results obtained from any kinetic theory referring to the isolated AP molecule could be compared directly with the experimental results. Evidence for the presence of intermolecular interactions that affect the proton dynamics in AP, in spite of the absence of dynamic solvent effects, was, however, obtained recently[58] by observing very small NH stretching band widths for crystalline AP, in contrast to broad bands characteristic for AP in liquid solution.

Effects of an Ordered Solid Environment. In order to learn more about this IR spectroscopically observed medium effect on the proton dynamics in AP we have performed the solid-state ^{15}N NMR experiments on crystalline AP described above. These experiments were interpreted in terms of the theoretical line shapes shown in Figure 3b, which indicate that the protons in crystalline AP at elevated temperatures move rapidly between the nitrogen

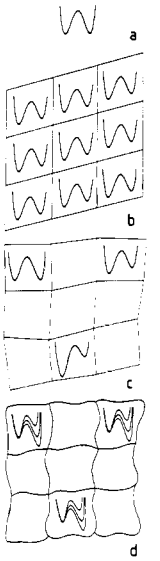

Figure 16. Perturbation of a symmetric double minimum potential of a bistable molecule by intermolecular interactions. (a) Symmetric double minimum potential in the gas phase; (b) perturbation of the potential in the ordered crystalline state by intermolecular interactions that are the same for all molecules; (c) perturbation of the potential in the disordered solid state by intermolecular interactions that are different for all molecules; (d) motional averaged symmetric potentials. (Adapted from ref 22.)

atoms, as shown in Figure 1. However, by contrast to the liquid, where—within the NMR time scale—the two tautomers in Figure 1 are of equal probability, their degeneracy appears to be lifted in the crystalline state because of time-independent intermolecular interactions. There is an energy difference ΔE of almost 12 kJ mol^{-1} between the two tautomeric states. The consequence is that even at 405 K the minor tautomer is populated to only ~5%. Model line shape calculations according to Figure 3b showed that because of this small population the dynamic line-broadening effects caused by moving from the slow- to the fast-exchange regime are too small to determine rate constants from the solid-state spectra. Note that in the solid state the molecules are fixed in space, i.e., there can be no reorientation around reacting molecules in order to stabilize polar transition states of zwitterions. The observation that the AP tautomerism is not quenched in the crystal but only perturbed is then consistent with the observation of the absence of dynamic solvent effects.

These findings are schematically modeled in Figure 16, parts a and b, where possible intermediates along the reaction pathway have been omitted for simplicity. The model, in fact, provides a general picture of how the symmetric gas-phase double minimum potential of bistable molecules is distorted in a crystal. Such a distortion will always arise when the reacting molecules are placed in a nonsymmetric way with respect to an existing preferential axis. In first approximation, the entropy difference ΔS between the two reactant states is still close to zero—as found here in the case of AP—and the reaction energy surface of one molecule will be independent of the molecular state of the neighboring molecules. In an ordered environment such as a crystal lattice, all molecules will then be characterized by the same energy difference $\Delta E \neq 0$ between the two wells of the double minimum potential (Figure 16b). Evidence for such solid-state effects has been found previously for different double proton transfer systems such as porphines and tetraaza[14]annulenes.[15-17,19-22] However, the magnitude of ΔE was much smaller in these cases as compared to azophenine. We will comment on this effect later. Since all molecules are equivalent in the crystal, they are all characterized by the same reaction energy surface and, therefore, by the same vibrational frequencies leading in the case of crystalline AP to sharp NH stretching bands.[58]

Effects of a Disordered Solid Environment. The much broader NH stretching band of AP in liquid CCl_4 then indicated a distribution of different solvation sites in which the AP molecules

experience slightly different NH stretching frequencies.[58] The question arises then whether the potential curves and, especially, the ΔE values of the tautomerism are also different in the different sites. This question is difficult to answer by either IR or by NMR spectroscopy. IR is not sensitive to ΔE, and only one averaged environment is observed by NMR. This is because the reorientation correlation times of molecules of the size of AP and, therefore, also the lifetimes of the different solvation sites are of the order of pico- to nanoseconds in the liquid state. Therefore, the different sites exchange rapidly as compared to the time scale of NMR spectroscopy and cannot be resolved by this method, in contrast to IR spectroscopy. However, this drawback could recently be overcome by studying fast proton transfers inside an organic tetraza[14]annulene dye, embedded in a disordered organic glass, by high-resolution solid-state ^{15}N NMR spectroscopy.[22] The tautomerism of the dye molecules was not suppressed in this system in spite of the slow molecular motions. By contrast, the latter were slow enough below the glass transition so that different solvation sites could be resolved. The ^{15}N NMR spectra were explained in terms of the model shown in Figure 16c. This model describes the fate of a symmetric double minimum potential of an isolated bistable molecule in disordered condensed media such as a glass or a liquid, in a time scale of slow molecular reorientation. The model assumes that the rearrangement between the two wells is still possible under these conditions. Because of the disorder of the environment the periodicity of the "unit cells" in which the bistable molecule is located has been lost, as is indicated schematically in Figure 16c. Depending on the environment, the molecules are distorted in different ways, leading to differently distorted double minimum potentials. Thus, it is understandable that the molecules in the different sites are not only characterized by different rate and equilibrium constants of the rearrangement but also by different frequencies of those vibrations coupled to the reaction coordinate. Environments with different equilibrium constants of dye tautomerism could be seen by NMR in the glassy state,[22] where the molecular motions are slow, i.e., where the lifetimes of the different environments are large. Above the glass transition, i.e., in the liquid state, the different molecular sites exchanged rapidly, leading to one motionally averaged apparently symmetric double minimum potential in the NMR time scale, as is illustrated schematically in Figure 16d.[22] However, the time scale of IR spectroscopy is so short that the molecular motions are not fast enough to average the different IR frequencies in the different sites. This explains the broad NH stretching bands of AP in liquid CCl_4 where for IR spectroscopy the situation has still to be described by Figure 16c.

Static Solvent Effect. It follows that the AP tautomerism in liquid solution is a very complicated process which can take place via a multitude of differently distorted double minimum potentials for the proton motion. In other words, a multitude of slightly different transition states has to be taken into account. The observed rate constants and the kinetic isotope effects are then motionally averaged values over different local environments. Thus, there is a "static" medium effect on the tautomerism, although there is no dynamic solvent effect in the sense that the latter must reorientate in order to enable the proton transfer. As stated above, our solid-state experiments indicate that an asymmetry of the double minimum potential of the proton motion does not hinder the protons from moving, in contrast to the predictions of coherent tunneling theories.[45-47]

Questions concerning the nature of the intermolecular interactios that perturb the proton transfer potential of AP, especially in the solid state, must be left open. These perturbations are quite substantial and, therefore, astonishing, in view of the fact that they are present even in apolar CCl_4. One can speculate that they might have something to do with possible phenyl group reorientations in AP. Let α_i be the angle between the phenyl group i and the molecular skeleton of AP. Because of steric hindrance, the different α_i values are, probably, not zero. This leads to an asymmetry of the AP reaction energy surface unless one assumes that the proton transfer potential is preceded or followed by a phenyl group reorientation. Whereas in the solid state the energy required to change the α_i is large, the corresponding energies for AP in the liquid state could be much smaller and could depend on the type of solvation site. Thus, it is conceivable that AP is characterized in liquid solution by a large distribution of angles α_i by contrast to the ordered crystalline state where all molecules experience the same set of angles. If the double minimum potential of the proton motion depends on the α_i it is understandable that the NH stretching frequencies also depend on these angles, which would explain the differential width of the corresponding bands in the liquid and the crystalline state.

Finally, note that in the case of ionic proton transfer or of electron-transfer reactions the perturbation of the potential energy surface by the environment will be much stronger than in the case of AP leading to large energy differences ΔE between the two potential wells in Figure 16. Then, the population of the well with the higher energy in a given site will be very small. However, when site exchange takes place the potential curve changes and this well will become dominantly populated. The consequence is that the reaction will be driven by the reorientation of the solute or solvent molecules; this then leads to strong dynamic solvent effects on the rate constants.

Conclusions

Various kinetic and spectroscopic experiments have been carried out in order to elucidate the mechanism of the proton tautomerism in azophenine (Figure 1). Although the two NH oscillators of AP are vibrationally coupled,[58] indicating that one hydrogen bond proton experiences the motion of the other in all stages of the reaction, the observed breakdown of the rule of the geometric mean for the kinetic HH/HD/DD isotope effects of the tautomerism is best explained with a stepwise proton transfer process involving two successive single proton transfers. The intermediate involved in this pathway (pathway c in Figure 13) has either a polar zwitterionic or an apolar structure, as expected for a singlet biradical. Because we do not find kinetic solvent effects in the range of dielectric constants between 2 and 25, the formation of a strongly solvated zwitterion is improbable. There is no evidence for strong tunnel contributions to the reaction rates; therefore, if tunneling is involved it must proceed from excited vibrational levels located just below the barrier of proton transfer. In the solid and, probably, also in the liquid the protons move rapidly along asymmetric double minimum potentials whose shapes depend on intermolecular interactions. As a consequence, there must be a substantial non-rate-determining heavy-atom motion in the liquid state, e.g., a phenyl group reorientation, solvation site exchange, etc., which precedes or follows the proton transfer and which restores the symmetry of the reaction energy surface within the NMR time scale. This heavy-atom motion is suppressed in the solid state. Thus, although solvent effects are small, the observed rate constants and kinetic isotope effects are affected by nonspecific solute–solvent interactions which are not easily taken into account. Further experimental and theoretical studies are necessary in order to solve the problem of kinetic isotope and solute–solvent solid-state effects in double proton transfer systems like AP in condensed phases.

Acknowledgment. We would like to thank Prof. M. M. Kreevoy, Minneapolis, MN, for stimulating discussions of the mechanism of the azophenine tautomerism. In addition, we thank him as well as Prof. R. L. Schowen, Lawrence, KS, and Prof. W. J. Albery, London, for their help in the development of the theory of kinetic isotope effects presented here. The financial support of the Deutsche Forschungsgemeinschaft, Bonn-Bad Godesberg, and the Fonds der Chemischen Industrie, Frankfurt, is gratefully acknowledged. The line shape calculations were performed on the Univac 1108 computer of the Rechenzentrum der Universität Freiburg i.Br.

Registry No. AP, 4435-12-5; H_2, 1333-74-0.